

OPTIMAL FEED TEMPERATURE FOR HYDROGEN PEROXIDE DECOMPOSITION PROCESS OCCURRING IN A BIOREACTOR WITH FIXED-BED OF COMMERCIAL CATALASE: A CASE STUDY ON THERMAL DEACTIVATION OF THE ENZYME

Ireneusz Grubecki*

UTP University of Science and Technology, Faculty of Chemical Technology and Engineering,
3 Seminaryjna Street, 85-326 Bydgoszcz, Poland

Dedicated to Professor Andrzej Burghardt on the occasion of his 90th birthday

On the basis of hydrogen peroxide decomposition process occurring in the bioreactor with fixed-bed of commercial catalase the optimal feed temperature was determined. This feed temperature was obtained by maximizing the time-average substrate conversion under constant feed flow rate and temperature constraints. In calculations, convection-diffusion-reaction immobilized enzyme fixed-bed bioreactor described by a coupled mass and energy balances as well as general kinetic equation for rate of enzyme deactivation was taken into consideration. This model is based on kinetic, hydrodynamic and mass-transfer parameters estimated in earlier work. The simulation showed that in the biotransformation with thermal deactivation of catalase optimal feed temperature is only affected by kinetic parameters for enzyme deactivation and decreases with increasing value of activation energy for deactivation. When catalase undergoes parallel deactivation the optimal feed temperature is strongly dependent on hydrogen peroxide feed concentration, feed flow rate and diffusional resistances expressed by biocatalyst effectiveness factor. It has been shown that the more significant diffusional resistances and the higher hydrogen peroxide conversions, the higher the optimal feed temperature is expected.

Keywords: fixed-bed (bio)reactor, hydrogen peroxide decomposition, optimal feed temperature, hydrogen peroxide conversion, parallel and thermal enzyme deactivation, diffusional resistances

1. INTRODUCTION

The use of immobilized enzymes is more advantageous than native ones, as it offers an easy product separation, increased thermal, chemical and operational stability of enzymes, protection against harmful environmental (mechanical or chemical) stress, and a better process control (Maria, 2012). In such cases the application of fixed-bed reactor (FXBR) seems to be a good choice. However, when working with immobilized enzymes internal and/or external diffusional resistances (IDR/EDR) are likely to occur regardless of the method of immobilization (Illanes, 2013). Thus, design and optimization of such reactors are not an easy task and often involve an inherent trade-off between different and conflicting objectives (Maria and

* Corresponding author, e-mail: ireneusz.grubecki@utp.edu.pl

Crisan, 2015). Particularly, in case of bioprocesses, optimal conditions assurance can be a very challenging task because of enzyme deactivation which is not always taken into account to properly predict a real bioreactor behavior. It should be noted that the factors responsible for enzyme deactivation characteristics in relationship to the main enzyme catalyzed reaction can be decisive in choosing the reactor operating mode and optimal operating strategy for the biotransformation course. It can be observed based on the application of catalase in the decomposition process of residual hydrogen peroxide (HP) (Farkye, 2004; Soares et al., 2011). In industrial practice hydrogen peroxide decomposition (HPD) usually is carried out under isothermal conditions at temperatures above 323 K (Horst et al., 2006), and at HP concentration lower or equal to $2 \times 10^{-2} \text{ kmol}\cdot\text{m}^{-3}$ (Costa et al., 2002). During this biotransformation usually deactivation of the catalase by the substrate is dominant. Nevertheless, at low concentrations of hydrogen peroxide (lower than $1.5 \times 10^{-3} \text{ kmol}\cdot\text{m}^{-3}$), and at temperatures above 308 K thermal deactivation could also be important (Miłek et al., 2014). Thus, feed HP concentration, and process temperature can adopt a crucial role in the course of enzyme deactivation. It is worth noting that the first factor is dependent on the course of industrial process in which hydrogen peroxide as a bleaching and bactericidal agent has been applied. Thus, the key problem is to determine the optimal temperature strategy adequate for the HPD process. This temperature strategy can be simply accomplished by searching for a suitable feed temperature that under a constant feed flow rate yields the maximum bioreactor productivity, and provides a compromise between the rate of reaction and that of (bio)catalyst deactivation. Analogical analysis was performed previously (Grubecki, 2018) for HPD process occurring in the presence of *Terminox Ultra* catalase (TUC) immobilized onto the non-porous glass beads and undergoing parallel deactivation. However, this analysis does not take into account the course of the HPD process at feed HP concentrations lower or equal to $1.5 \times 10^{-3} \text{ kmol}\cdot\text{m}^{-3}$, and consequently the selection of optimal feed temperature (OFT) for the HPD by TUC undergoing the thermal deactivation.

Hence, the objective of the present study was to search for the OFT of the fixed-bed bioreactor for HPD process occurring in the presence of immobilized TUC undergoing thermal deactivation (independent of substrate concentration), and in the light of the previous analysis (Grubecki, 2018) to determine the effect of enzyme deactivation mechanism on optimal strategy under consideration. The optimal feed temperature has been achieved by maximizing time-averaged substrate conversion accounting for the lower and the upper temperature constraints as well as diffusional resistances expressed by the global effectiveness factor.

The analysis presented here is a continuation and generalization of considerations reported previously (Grubecki, 2018). It offers an insight into the majority of the continuous processes with enzyme deactivation independent of the substrate concentration that could be encountered in industrial practice.

2. MATHEMATICAL PROBLEM APPROACH

2.1. Kinetic rate equations for reaction and enzyme deactivation

The rate of changes in substrate concentration (r_S) of any enzymatic reaction running in the presence of immobilized enzyme, especially HPD, can be described by the classical Michaelis-Menten kinetics (Ogura, 1955)

$$r_S = \eta_{\text{eff}} k'_R(T) \frac{C_E C_S}{(1 + C_S/K_M)} \quad (1)$$

Each biotransformation is accompanied by diminishing activity of biocatalyst, the rate of which as a function of substrate concentration (Vasudevan and Weiland, 1990) and temperature can be expressed in the form

$$-\frac{dC_E}{dt} = \left[\eta_{\text{eff}} \frac{C_S}{(1 + C_S/K_D)} \right]^q k_D(T) C_E \quad (2)$$

Equation (2) describes the rate of enzyme deactivation both independent of ($q = 0$, thermal deactivation) and dependent on substrate concentration ($q = 1$, parallel deactivation), and particularly can be related to thermal deactivation of catalase (Miłek et al., 2014) as well as deactivation of catalase by hydrogen peroxide, respectively. The simple model of thermal catalase deactivation (Eq. (2) for $q = 0$) accounts for the complexity of the enzyme molecule and has been validated for such enzymes as glycosylases (Ricca et al., 2009; Shao-Wei and Da-Nian, 2008), proteases (Katsaros et al., 2009a; 2009b; Wilińska et al., 2008), and more (Mohapatra et al., 2007; Naidu and Panda, 2003).

2.2. Fixed-bed (bio)reactor model

A schematic diagram of fixed-bed bioreactor for HPD process and its characteristics are shown in Fig. 1.

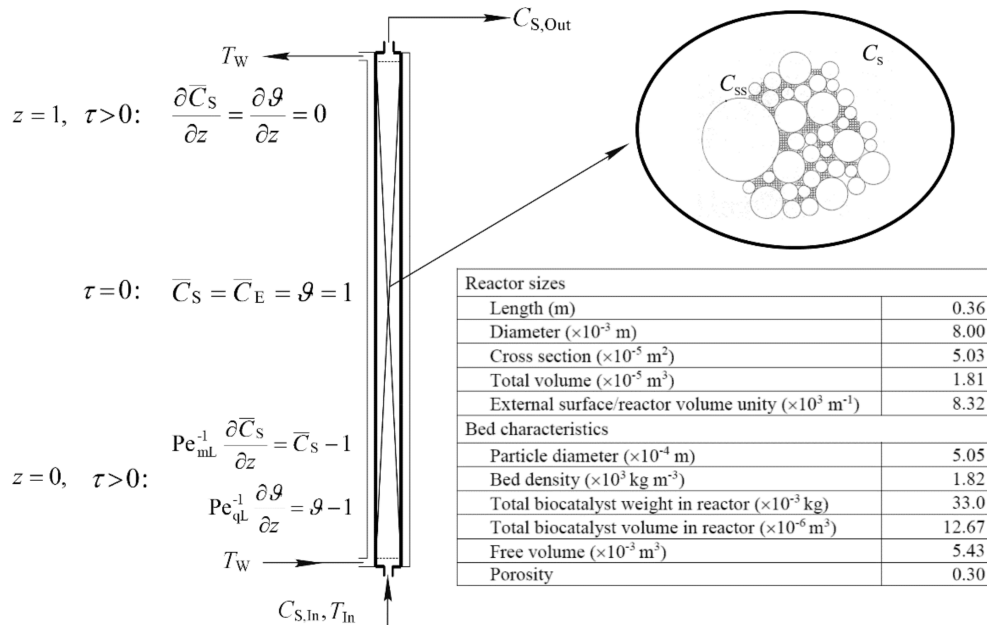


Fig. 1. Schematic diagram of fixed-bed bioreactor for HPD process with initial and boundary conditions

To formulate and then solve the mathematical model of FXBR in which the HPD by immobilized TUC is carried out the following assumptions have been made: 1) catalyst particles are spherical and uniformly packed inside the reactor, 2) volume and density of the reacting medium are constant, 3) the effective diffusivity does not change throughout the particles and is independent of the HP concentration, 4) process is diffusion-controlled, 5) the feed and pellet temperatures remain constant, 6) the radial concentration and temperature gradients in the bulk liquid are assumed to be negligible, 7) in industrial practice HPD is carried out at low HP concentration (lower or equal to $0.02 \text{ kmol}\cdot\text{m}^{-3}$), therefore, it can be assumed that $C_s \ll K_M$ and $C_s \ll K_D$, 8) substrate (HP) transport rate (r_m) from the bulk liquid (C_S) to the outer surface of the immobilized bead (C_{SS}) is equimolar diffusion described by the Eq. (3)

$$r_m = k_{mL} a_m (C_S - C_{SS}) \quad (3)$$

2.2.1. Mass and energy balances with enzyme deactivation rate equation

Accounting for the above assumptions and introducing dimensionless state variables

$$\bar{C}_E = \frac{C_E}{C_{E0}}, \quad \bar{C}_S = \frac{C_S}{C_{S,In}}, \quad \vartheta = \frac{T}{T_{In}} \quad (4)$$

dimensionless axial coordinate variable (z) and dimensionless biocatalyst age (τ)

$$z = \frac{h}{H}, \quad \tau = t \frac{U_S}{H} \quad (5)$$

as well as dimensionless process parameters

$$Pe_{mL} = \frac{U_S H}{\varepsilon D_L}, \quad Pe_{qL} = \frac{\rho C_P U_S H}{\varepsilon \Lambda_x}, \quad St_H = \frac{4\alpha_W}{D_R \rho C_P} \frac{H}{U_S} \quad (6a)$$

$$K_1 = k_R a_m \frac{H}{U_S}, \quad K_2 = k_D C_{S,In}^q \frac{H}{U_S} \quad (6b)$$

$$H_R = \frac{(-\Delta H_R) C_{S,In}}{\rho C_P T_{In}}, \quad \beta_i = \frac{E_i}{RT_{In}} \quad (i = D, R) \quad (6c)$$

the mathematical expressions of the mass and energy balances in the bulk liquid phase as well as equation for the enzyme deactivation rate describing the course of HPD process in fixed-bed bioreactor with external heat exchange can be written in the form of Eqs. (7)–(9)

$$\varepsilon \frac{\partial \bar{C}_S}{\partial \tau} = Pe_{mL}^{-1} \frac{\partial^2 \bar{C}_S}{\partial z^2} - \frac{\partial \bar{C}_S}{\partial z} - \eta_{eff}(1 - \varepsilon) K_1 \bar{C}_E \bar{C}_S \quad (7)$$

$$\varepsilon \frac{\partial \vartheta}{\partial \tau} = Pe_{qL}^{-1} \frac{\partial^2 \vartheta}{\partial z^2} - \frac{\partial \vartheta}{\partial z} + St_H(\vartheta_W - \vartheta) - \eta_{eff}(1 - \varepsilon) K_1 H_R \bar{C}_E \bar{C}_S \quad (8)$$

$$-\frac{\partial \bar{C}_E}{\partial \tau} = (1 - \varepsilon)(\eta_{eff} \bar{C}_S)^q K_2 \bar{C}_E \quad (9)$$

The initial ($\tau = 0$) and boundary conditions for Eqs. (7)–(9) at the entry ($z = 0$) and the exit ($z = 1$) of the (bio)reactor are illustrated in Fig. 1.

The formulated mathematical model allows to predict the real behavior of the fixed-bed bioreactor for HPD process occurring in the presence of commercial catalase in industrial practice.

2.2.2. Evaluation of the effectiveness factor

It has been mentioned that when working with immobilized enzymes diffusional resistances are likely to occur and can be expressed by effectiveness factor. Moreover, it was proved (Grubecki, 2017) that in the HPD process occurring in the presence of immobilized TUC the EDR should not be neglected. Then, to properly assess real bioreactor behavior, the global effectiveness factor ($\eta_{eff} = \eta_G$) appearing in Eqs. (1), (2) and (7)–(9) should be introduced (Maria and Crisan, 2015)

$$\eta_G = \frac{Bi [\tanh^{-1}(3\phi) - (3\phi)^{-1}]}{\phi [Bi - 1 + 3\phi \tanh^{-1}(3\phi)]} \quad (10)$$

where Bi and ϕ represent the Biot number and Thiele modulus for biochemical reaction of first-order kinetics, respectively, and calculated using external mass-transfer model developed previously (Grubecki, 2017) as well as kinetic parameters for reaction and deactivation describing the process free of diffusional resistances. Behavior of the effectiveness factors under EDR and the combined effect of EDR and IDR (Eq. (10)) have been described elsewhere (Grubecki, 2018).

2.2.3. Estimation of film mass transfer coefficient

External mass transfer limitations have a significant effect on the performance of immobilized enzyme reactor for HPD. Thus, to predict the mass-transfer coefficient (k_{mL}) for HP the correlation developed by Chilton and Colburn (1934) and experimentally verified by Grubecki (2017) was used

$$k_{mL} = K \frac{D_{L,S}^{2/3}}{d_P^{1-n}} \left(\frac{\rho}{\eta} \right)^{(n-1/3)} U_S^n \quad (11)$$

with n and K values assessed to be equal to 0.632 and 0.972, respectively. Equation (11) is applicable for $0 < Re < 20$.

2.3. Optimization

2.3.1. Performance index

An optimizing problem has been formulated as a searching for the feed temperature that under constant feed flow rate would provide maximum time-averaged HP conversion

$$\alpha_m = \frac{1}{\tau_f} \int_0^{\tau_f} [1 - \bar{C}_S(z=1, x)] dx \quad (12)$$

To ensure safe operation the process temperature and feed flow rate, Q , are bounded as below

$$\vartheta_{\min} \leq \vartheta \leq \vartheta_{\max} \quad \text{and} \quad Q_{\min} \leq Q \leq Q_{\max} \quad (13)$$

2.3.2. Optimization calculus

The optimal feed temperature maximizing the time-averaged HP conversion was obtained using constrained non-linear minimization with MATLAB Optimization Toolbox (Mathworks Inc., Natick MA, USA). In optimization procedure the MATLAB PDE Toolbox was employed to solve a set of non-linear partial differential equations (Eqs. (7)–(9)).

3. OPTIMIZATION RESULTS

To perform the calculations the kinetic parameters for reaction and enzyme parallel deactivation determined earlier (Grubecki, 2017) from data collected during a laboratory study for the process of HPD by TUC immobilized onto non-porous glass beads running in the model reactor were adopted. Activation energy and frequency factor for thermal deactivation of catalase with the commercial name *Terminox Ultra* were $140.93 \pm 0.63 \text{ kJ}\cdot\text{mol}^{-1}$ and $(3.21 \pm 0.87) \times 10^{17} \text{ s}^{-1}$, respectively (Miłek et al., 2014).

Péclet numbers for mass Pe_{mL} and heat Pe_{qL} transfer, effective diffusion coefficient D_{eff} as well as the other parameters necessary to perform the calculations have been described earlier (Grubecki, 2018). Moreover, in the computations the heat transfer coefficient between wall and bulk liquid phase of

$\alpha_w = 330 \text{ W}\cdot\text{m}^{-2}\cdot\text{K}^{-1}$ calculated according to the correlation of Dixona and Cresswell (1979) as well as the jacket fluid temperature corresponding to the feed temperature were adopted.

The effect of the feed flow rate, Q , and feed temperature, T_{In} , on the changes of time-average HP conversion (Eq. (12)) at the bioreactor outlet in the HPD process with thermal deactivation (solid lines) and parallel one (dasched lines) has been shown in Fig. 2.

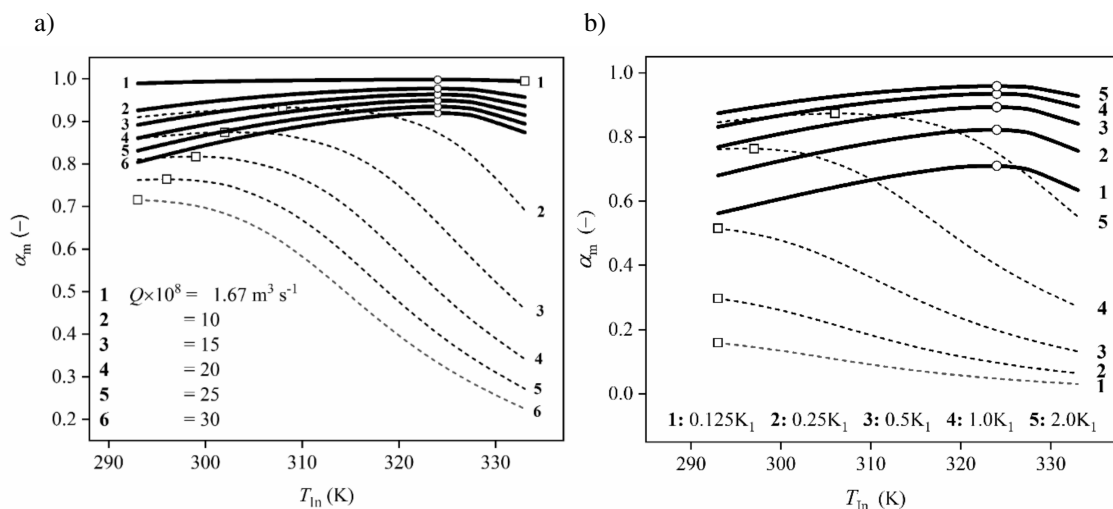


Fig. 2. The effect of the feed temperature (T_{In}) and a) feed flow rate (Q), b) initial enzyme activity expressed by K_1 parameter value on time-average HP conversion at the reactor outlet in the HPD process with thermal deactivation of catalase (solid lines) for $C_{S,In} = 5 \times 10^{-4} \text{ kmol}\cdot\text{m}^{-3}$ and parallel one (dashed lines) for $C_{S,In} = 5 \times 10^{-3} \text{ kmol}\cdot\text{m}^{-3}$. Open symbols (\circ for $q = 0$, \square for $q = 1$) represent the maximum values of time-average HP conversion. Line 1 on the left represents the dependences α_m vs T_{In} for both analyzed deactivation mechanisms

In the decomposition process of hydrogen peroxide with catalase deactivation both independent of and dependent on HP concentration – for the analyzed values of kinetic and mass-transfer parameters – the feed temperature can be indicated, which maximizes the time-average HP conversion at the reactor outlet. The higher the difference between the upper and the lower permissible temperatures, the more OFT is likely to occur.

In the process with thermal TUC deactivation ($q = 0$, Fig. 2, solid lines) the OFT is independent of feed flow rate (at the same time EDR associated with diffusional transport through the stagnant layer surrounding the solid biocatalyst particle), internal diffusional resistances (IDR), and consequently combined effect EDR and IDR (Fig. 3) as well as feed HP concentration and initial enzyme activity (Fig. 2b). Moreover, the lower the feed flow rate, the more significant global diffusional resistances and the higher time-average HP conversion. It should be noted that the OFT is closely related to the value of activation energy for thermal deactivation, E_D . The higher the E_D value, the faster the enzyme deactivation at higher temperature, and consequently, the lower conversion. Therefore, the lower OFT is required (Fig. 4).

As proved previously (Grubecki, 2018), in biotransformation with parallel TUC deactivation ($q = 1$, Fig. 2, dashed lines) the opposite situation appears. Namely, the OFT is closely related to the feed flow rate and to effectiveness factor at the same time. This means that the OFT exists only for a certain value (at least one) of the feed flow rate Q^\bullet . For the feed flow rates higher than Q^\bullet ($Q > Q^\bullet$), time-average HP conversion decreases with raising temperature T_{In} , and then the OFT becomes equal to the lower permissible temperature. On the contrary, for the feed flow rates lower than Q^\bullet ($Q < Q^\bullet$), average HP conversion increases with the raising temperature, and the OFT should be equal to the upper temperature constraint. Thus, there exists such a feed temperature for which the time-average HP conversion is at its maximum. Based in Fig. 2 it can be said that the selection of unsuitable temperature makes the HPD process with parallel TUC deactivation less efficient than the process with thermal one.

In the hydrogen peroxide decomposition process by TUC undergoing the thermal deactivation the OFT is equal to 324 K (Fig. 2–4) for all feed flow rates under considerations with time-average HP conversions at the bioreactor outlet remaining $\alpha_m = 0.934$ for $Q^\bullet = 25 \times 10^{-8} \text{ m}^3 \cdot \text{s}^{-1}$ corresponding to a value of $\eta_G^\bullet = 0.220$, $\alpha_m = 0.948$ for $Q^\bullet = 20 \times 10^{-8} \text{ m}^3 \cdot \text{s}^{-1}$ corresponding to a value of $\eta_G^\bullet = 0.208$, $\alpha_m = 0.963$ for $Q^\bullet = 15 \times 10^{-8} \text{ m}^3 \cdot \text{s}^{-1}$ corresponding to a value of $\eta_G^\bullet = 0.191$, and $\alpha_m = 0.977$ for $Q^\bullet = 10 \times 10^{-8} \text{ m}^3 \cdot \text{s}^{-1}$ corresponding to a value of $\eta_G^\bullet = 0.167$.

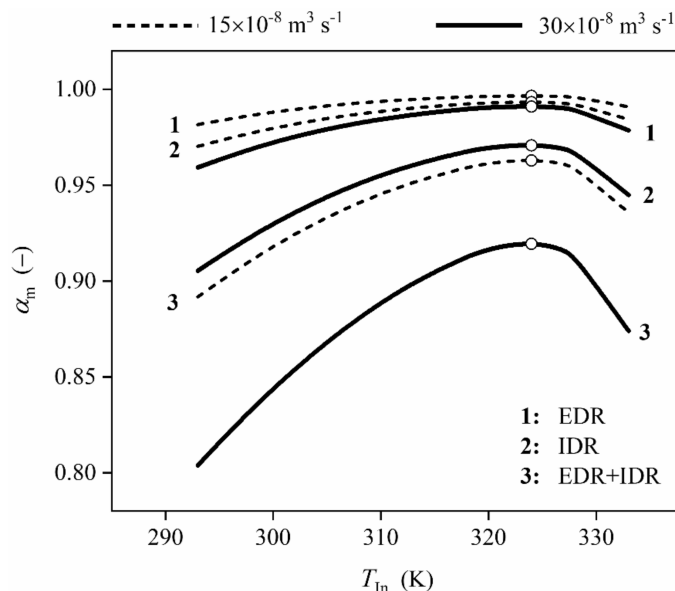


Fig. 3. The effect of feed temperature and diffusional resistances on OFT in the HPD with thermal deactivation of catalase. Open symbols represent the maximum values of time-average HP conversion

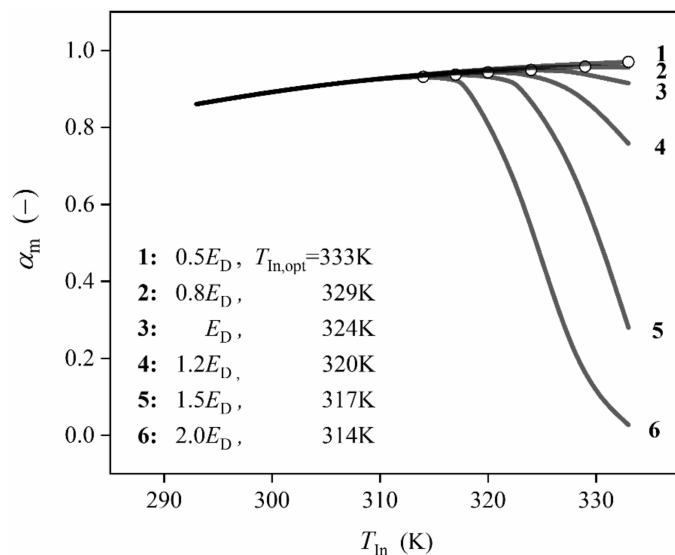


Fig. 4. The effect of feed temperature and activation energy for thermal deactivation on OFT for $Q = 25 \times 10^{-8} \text{ m}^3 \cdot \text{s}^{-1}$. Open symbols represent the maximum values of time-average HP conversion

For HPD process with parallel deactivation the feed flow rates (Q^\bullet) for maximum conversions of HP are equal to: $Q^\bullet = 25 \times 10^{-8} \text{ m}^3 \cdot \text{s}^{-1}$ corresponding to a value of $\eta_G^\bullet = 0.210$ with $\alpha_m = 0.764$, $Q^\bullet = 20 \times 10^{-8} \text{ m}^3 \cdot \text{s}^{-1}$ corresponding to a value of $\eta_G^\bullet = 0.198$ with $\alpha_m = 0.817$, $Q^\bullet = 15 \times 10^{-8} \text{ m}^3 \cdot \text{s}^{-1}$

corresponding to a value of $\eta_G^\bullet = 0.181$ with $\alpha_m = 0.874$, $Q^\bullet = 10 \times 10^{-8} \text{ m}^3 \cdot \text{s}^{-1}$ with $\eta_G^\bullet = 0.159$ and $\alpha_m = 0.932$. For $Q \geq Q^\bullet$ (in this case $Q \geq 30 \times 10^{-8} \text{ m}^3 \cdot \text{s}^{-1}$), the average HP conversion decreases with temperature rise and then, the OFT corresponds to the lower allowable temperature ($T_{\text{In,opt}} = T_{\text{min}}$). For $Q \leq Q^\bullet$ (in this case $Q \leq 1.67 \times 10^{-8} \text{ m}^3 \cdot \text{s}^{-1}$) the average HP conversion increases when feed temperature (T_{In}) grows, and then the OFT equals the upper allowable temperature ($T_{\text{In,opt}} = T_{\text{max}}$).

It is obvious that application of the biocatalyst with larger size results in the rise of the diffusional resistances, and consequently the decrease of the global effectiveness factor. As a result, the OFT is expected to be increased in HPD process with parallel TUC deactivation (Grubecki, 2018) or remains constant in the process with thermal one.

A similar situation appears when the effect of external film diffusion can be disregarded. Then the process course can be controlled only by IDR related to the mass-transport of HP inside the pores of the support and independent of the feed flow rate (Q). In such a case the OFT ensuring the maximum time-average HP conversion should reach the lower value than that required in the biotransformation with global mass-transport of HP, when enzyme undergoes parallel deactivation, or takes a fixed value in the process with thermal one.

4. CONCLUSIONS

Based on the presented simulation study carried out for parametric values the following conclusions can be drawn:

- In any fixed-bed reactor, especially in a bioreactor for HPD with fixed-bed of commercial catalase, a certain value of the feed temperature can be indicated for which the time-average substrate conversion attains the maximum or is the highest. In the biotransformations with thermal deactivation of catalase this feed temperature is only affected by the activation energy for deactivation, and with a rising value of energy the OFT decreases. In HPD process with parallel deactivation of TUC, the OFT is strongly dependent on diffusional resistances, feed HP concentration, and enzyme activity. The higher diffusional resistances (the lower value of effectiveness factor), the lower the feed HP concentration, and the higher enzyme activity, the higher the temperature that yields the maximum (or the highest) level of the time-average HP conversion at the reactor outlet.
- Hydrogen peroxide conversions predicted in the HPD process with thermal deactivation of catalase are higher than those expected for HPD with parallel deactivation, while relative increase of conversions diminishes when feed flow rate decreases and varies from 35% for $Q = 50 \times 10^{-8} \text{ m}^3 \cdot \text{s}^{-1}$ to 0.2% for $Q = 3.33 \times 10^{-8} \text{ m}^3 \cdot \text{s}^{-1}$.
- The results obtained in this work can be indispensable to scale up bioreactors for hydrogen peroxide decomposition without prior estimation of kinetic and process parameters required to select operating conditions for which the productivity of the bioreactor under consideration attains the maximum or is the highest.

SYMBOLS

a_m	external surface area for mass transfer, $\text{m}^2 \cdot \text{m}^{-3}$
Bi	Biot number ($= k_{mL} d_p / 6D_{\text{eff}}$)
C_E	enzyme activity, $\text{kg} \cdot \text{m}^{-3}$
C_p	heat capacity for the bulk liquid, $\text{J} \cdot \text{kg}^{-1} \cdot \text{K}^{-1}$

C_S	bulk substrate concentration, $\text{kmol}\cdot\text{m}^{-3}$
$C_{S,j}$	H_2O_2 concentration at the inlet ($j = \text{In}$) and outlet ($j = \text{Out}$), $\text{kmol}\cdot\text{m}^{-3}$
d_P	particle diameter, m
D_{eff}	effective diffusion coefficient, $\text{m}^2\cdot\text{s}^{-1}$
D_f	substrate diffusivity, $\text{m}^2\cdot\text{s}^{-1}$
D_L	axial dispersion coefficient, $\text{m}^2\cdot\text{s}^{-1}$
D_R	reactor diameter, respectively, m
E_i	activation energy for reaction ($i = \text{R}$) and deactivation ($i = \text{D}$), $\text{J}\cdot\text{mol}^{-1}$
h	distance from reactor inlet, m
H	bed depth, m
H_R	dimensionless heat of reaction ($= (-\Delta H_R)C_{S,\text{In}}/\rho C_P T_{\text{In}}$)
$-\Delta H_R$	heat of reaction, $\text{J}\cdot\text{mol}^{-1}$
k_D	modified rate constant for deactivation ($= v_D/K_D$), $\text{m}^3\cdot\text{kmol}^{-1}\cdot\text{s}^{-1}$
k_{D0}	pre-exponential factor for deactivation rate constant, $\text{m}^3\cdot\text{kmol}^{-1}\cdot\text{s}^{-1}$
k_{mL}	mass transfer coefficient, $\text{m}\cdot\text{s}^{-1}$
k'_R	modified rate constant for reaction ($= v_R/K_M$), $\text{m}^3\cdot\text{kg}^{-1}\cdot\text{s}^{-1}$
k_{R0}	pre-exponential factor for enzymatic reaction rate constant, $\text{m}\cdot\text{s}^{-1}$
k_R	modified rate constant for reaction ($= k'_R C_{E0}/a_m$), $\text{m}\cdot\text{s}^{-1}$
K_1	dimensionless number ($= k_R a_m H/U_S$)
K_2	dimensionless number ($= k_D C_{S,\text{In}} H/U_S$)
K_i	Michaelis constant for reaction ($i = \text{R}$) and deactivation ($i = \text{D}$), $\text{kmol}\cdot\text{m}^{-3}$
Pe_{mL}	Péclet number for mass transfer ($= U_S H/\varepsilon D_L$)
Pe_{qL}	Péclet number for heat transfer ($= \rho C_P U_S H/\varepsilon \Lambda_x$)
Q	feed flow rate, $\text{m}^3\cdot\text{s}^{-1}$
r_m	mass transfer rate, $\text{kmol}\cdot\text{m}^{-3}\cdot\text{s}^{-1}$
r_S	reaction rate, $\text{kmol}\cdot\text{m}^{-3}\cdot\text{s}^{-1}$
St_H	Stanton number ($= 4\alpha_w H/D_R \rho C_P U_S$)
t	biocatalyst age, s
T_{In}	feed temperature, K
$T_{\text{min}}, T_{\text{max}}$	lower and upper temperature constraints, K
U_S	superficial velocity, $\text{m}\cdot\text{s}^{-1}$
z	dimensionless distance from reactor inlet ($= h/H$)

Greek letters

α_m	time-average substrate conversion
α_w	heat-transfer coefficient, $\text{W}\cdot\text{m}^{-2}\cdot\text{K}^{-1}$
β_i	dimensionless Arrhenius number defined as (E_i/RT_{In}) ($i = \text{D}, \text{R}$)
ε	porosity of the porous medium ($= 0.3$)
ϕ	Thiele modulus ($= d_P/(k_R a_m/D_{\text{eff}})^{0.5}$)
η	fluid viscosity, $\text{kg}\cdot\text{m}^{-1}\cdot\text{s}^{-1}$
η_{eff}	effectiveness factor defined by Eqs. (10)
Λ_x	axial heat conduction in liquid phase, $\text{W}\cdot\text{m}^{-1}\cdot\text{K}^{-1}$
λ	liquid thermal conductance, $\text{W}\cdot\text{m}^{-1}\cdot\text{K}^{-1}$
v_D	rate constant for deactivation, s^{-1}
v_R	rate constant for reaction, $\text{kmol}\cdot\text{kg}^{-1}\cdot\text{s}^{-1}$
ρ	liquid density, $\text{kg}\cdot\text{m}^{-3}$
τ	dimensionless time ($= tU_S/H$)
ϑ	dimensionless state variable ($= T/T_{\text{In}}$)

Abbreviations

CAT	Catalase
FXBR	Fixed-Bed Reactor
EDR	External Diffusional Resistances
HP	Hydrogen Peroxide
HPD	Hydrogen Peroxide Decomposition
IDR	Internal Diffusional Resistances
OFT	Optimal Feed Temperature
PDE	Partial Differential Equations
TUC	<i>Terminox Ultra</i> Catalase

REFERENCES

- Chilton T.H., Colburn A.P., 1934. Mass transfer (absorption) coefficients predictions from data on heat transfer and fluid friction. *Ind. Eng. Chem.*, 26, 1183–1187. DOI: 10.1021/ie50299a012.
- Costa S.A., Tzanov T., Carneiro F., Gubitz G.M., Cavaco-Paulo A., 2002. Recycling of textile bleaching effluents for dyeing using immobilized catalase. *Biotechnol. Lett.*, 24, 173–176. DOI: 10.1023/a:1014136703369.
- Dixon A.G., Cresswell D.L., 1979. Theoretical prediction of effective heat transfer parameters in packed beds. *AIChE J.*, 25, 663–676. DOI: 10.1002/aic.690250413.
- Farkye N.Y., 2004. Cheese technology. *Int. J. Dairy Technol.*, 57, 91–98. DOI: 10.1111/j.1471-0307.2004.00146.x.
- Grubecki I., 2018. Optimal feed temperature for an immobilized enzyme fixed-bed bioreactor: A case study on hydrogen peroxide decomposition by commercial catalase. *Chem. Process Eng.*, 39, 39–57. DOI: 10.24425/119098.
- Grubecki I., 2017. External mass transfer model for hydrogen peroxide decomposition by *Terminox Ultra* catalase in a packed-bed reactor. *Chem. Process Eng.*, 38, 307–319. DOI: 10.1515/cpe-2017-0024.
- Horst F., Rueda E.H., Ferreira M.L., 2006. Activity of magnetite-immobilized catalase in hydrogen peroxide decomposition. *Enzyme Microb. Technol.*, 38, 1005–1012. DOI: 10.1016/j.enzmictec.2005.08.035.
- Illanes A. (Eds.), 2013. Enzyme reactor design and operation under mass-transfer limitations, In: *Problem solving in enzyme biocatalysis*. John Wiley and Sons Ltd, 181–202.
- Katsaros G.I., Katapodis P., Taoukis P.S., 2009a. High hydrostatic pressure inactivation kinetics of the plant proteases ficin and papain. *J. Food Eng.*, 91, 42–48. DOI: 10.1016/j.jfoodeng.2008.08.002.
- Katsaros G.I., Katapodis P., Taoukis P.S., 2009b. Modeling the effect of temperature and high hydrostatic pressure on the proteolytic activity of kiwi fruit juice. *J. Food Eng.*, 94, 40–45. DOI: 10.1016/j.jfoodeng.2009.02.026.
- Maria G., 2012. Enzymatic reactor selection and derivation of the optimal operation policy, by using a model-based modular simulation platform. *Comput. Chem. Eng.*, 36, 325–341. DOI: 10.1016/j.compchemeng.2011.06.006.
- Maria G., Crisan M., 2015. Evaluation of optimal operation alternatives of reactors used for d-glucose oxidation in a bi-enzymatic system with a complex deactivation kinetics. *Asia-Pac. J. Chem. Eng.*, 10, 22–44. DOI: 10.1002/apj.1825.
- Milek J., Wójcik M., Verschelde W., 2014. Thermal stability for the effective use of commercial catalase. *Polish J. Chem. Technol.*, 16, 75–79. DOI: 10.2478/pjct-2014-0073.
- Mohapatra B.R., Douglas Gould W., Dinardo O., Papavinasam S., Koren D.W., Winston Revie R., 2007. Effect of immobilization on kinetic and thermodynamic characteristics of sulfide oxidase from arthrobacter species. *Prep. Biochem. Biotechnol.*, 38, 61–73. DOI: 10.1080/10826060701774361.
- Naidu G.S.N., Panda T., 2003. Studies on pH and thermal deactivation of pectolytic enzymes from *Aspergillus niger*. *Biochem. Eng. J.*, 16, 57–67. DOI: 10.1016/S1369-703X(03)00022-6.
- Ogura Y., 1955. Catalase activity at high concentration of hydrogen peroxide. *Arch. Biochem. Biophys.*, 57, 288–300. DOI: 10.1016/0003-9861(55)90291-5.

- Ricca E., Calabro, V., Curcio S., Iorio G., 2009. Optimization of inulin hydrolysis by inulinase accounting for enzyme time- and temperature-dependent deactivation. *Biochem. Eng. J.*, 48, 81–86. DOI: 10.1016/j.bej.2009.08.009.
- Shao-Wei D., Da-Nian L., 2008. Kinetics of the thermal inactivation of *Bacillus subtilis* α -amylase and its application on the desizing of cotton fabrics. *J. Appl. Polym. Sci.*, 109, 3733–3738. DOI: 10.1002/app.28612.
- Soares J.C., Moreira P.R., Queiroga A.C., Morgado J., Malcata F.X., Pintado M.E., 2011. Application of immobilized enzyme technologies for the textile industry: A review. *Biocatal. Biotransform.*, 29, 223–237. DOI: 10.3109/10242422.2011.635301.
- Vasudevan P.T., Weiland R.H., 1990. Deactivation of catalase by hydrogen peroxide. *Biotechnol. Bioeng.*, 36, 783–789. DOI: 10.1002/bit.260360805.
- Wilińska A., de Figueiredo Rodrigues A.S., Bryjak J., Polakovič M., 2008. Thermal inactivation of exogenous pectin methylesterase in apple and cloudberry juices. *J. Food Eng.*, 85, 459–465. DOI: 10.1016/j.jfoodeng.2007.08.009.

Received 29 August 2018

Received in revised form 22 October 2018

Accepted 23 October 2018